Supplementary Information

Perylene-based Aromatic Polyimide with Multiple Carbonyls Enabling High-Capacity and Stable Organic Lithium and Sodium Batteries

*Michael Ruby Raj, Nangyeong Kim, and Gibaek Lee**

Advanced Energy Materials Design Lab, Chemical Engineering for Energy, School of Chemical Engineering, Yeungnam University, 38541 Gyeongsan-Si, Republic of Korea.

*Corresponding author

E-mail: gibaek@ynu.ac.kr (Prof. Gibaek Lee).

Contents

Figure S8. SEM images of (a, b) the pristine PI electrodes; (c, d) cycled PI electrodes for Li^+/Li; and (e, f) cycled PI electrodes for Na^+/Na. Approximately 1000 cycles were conducted at 200 mA g^{-1}.

Figure S9. Ex-situ XPS local-scan spectra of N 1s regions for the different states of the PI electrodes (for Li^+/Li and Na^+/Na) after charging to 3.5 V and discharging to 1.5V.

Table S1. Summary of electrolyte resistance (R_e), charge transfer resistance (R_{ct}) for fresh and tested cells at different cycle numbers in both PI-based LIBs and SIBs.

1. Synthetic procedure for the synthesis of perylene-based aromatic polyimide (PI) through polymerization of perylene-3,4:9,10-tetracarboxylic acid (PTCDA) units with 2,6-diaminoanthraquinone (2,6-DAAQ) in a single condensation reaction step (as shown in Scheme 1).

The mixture of PTCDA units (2 g, 5.1 mmol) and 50 g of imidazole was heated and stirring at 150 °C under a nitrogen atmosphere for the complete dissolution of the starting material. Subsequently, 2,6-DAAQ (1.2 g, 5.04 mmol) was added gradually (portion-wise) to this mixture at 150 °C. The reaction mixture was gradually heated to 165–170 °C and maintained at the same temperature for 24 h. Subsequently, it was cooled to 60 °C, and methanol (100 mL) was added into the reaction mixture under stirring to precipitate the product. The black precipitate was collected through vacuum filtration and was washed with DMF (2×50 mL) and ethanol (2×100 mL). The final product was collected as a black powder (2.9 g, 95.7%). The decomposition temperature based on 5% weight loss by TGA was 286 °C; FT-IR (KBr): ν = 1698 (s), 1663 (s), 1587 (s), 1571 (s), 1340 (br), 737 cm^{-1} (br). Solid-state ^{13}C CP/MAS NMR (125 Hz) δ: 181.75 (C=O), 178.67 (C=O), 161.63 (C=O), 154.05, (Ar-C) 141.91 (Ar-C), 133.50 (Ar-C), 130.76 (Ar-C), 120.90 (Ar-C), 107.81 (Ar-C) ppm. Anal. calcd. for $(C_{38}H_{14}N_2O_6)_n$: C, 76.77; H, 2.37; N, 4.70; O, 16.09%; found: C, 76.25; H, 2.41; N, 4.78%.

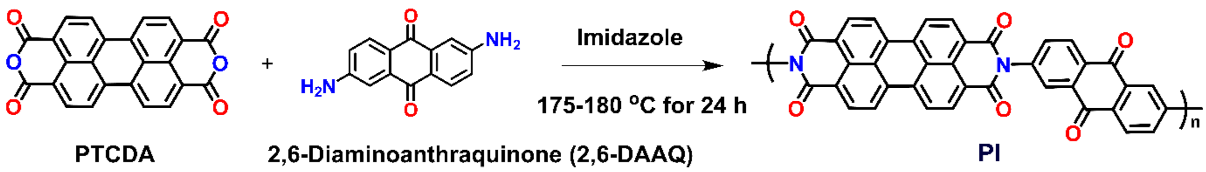

Scheme S1. Synthetic method for the synthesis of perylene-based aromatic polyimide (**PI**) through polymerization of a PTCDA unit with 2,6-DAAQ in a single condensation step.

Theoretical capacity calculation:

The theoretical capacity (***C_{spec}***) of **PI** was calculated based on a three-electron transfer redox process for each formula unit of **PI** using the given equation:

$$\boldsymbol{C_{spec}} = \frac{n\ X\ 96485.332\ (mAh)}{3.6\ \mathrm{X}\ \mathrm{Mw}\ (g)} = \frac{26801\ (mAh)}{\mathrm{Mw\ (g)}} = \mathbf{135.24\ mAh\ g^{-1}}$$

Where n = 3 and Mw is the molecular weight is about 594.5 g/mole for the single unit of **PI**.

Figure S1. Solid-state ^{13}C CP/MAS NMR spectrum of polyimide (PI).

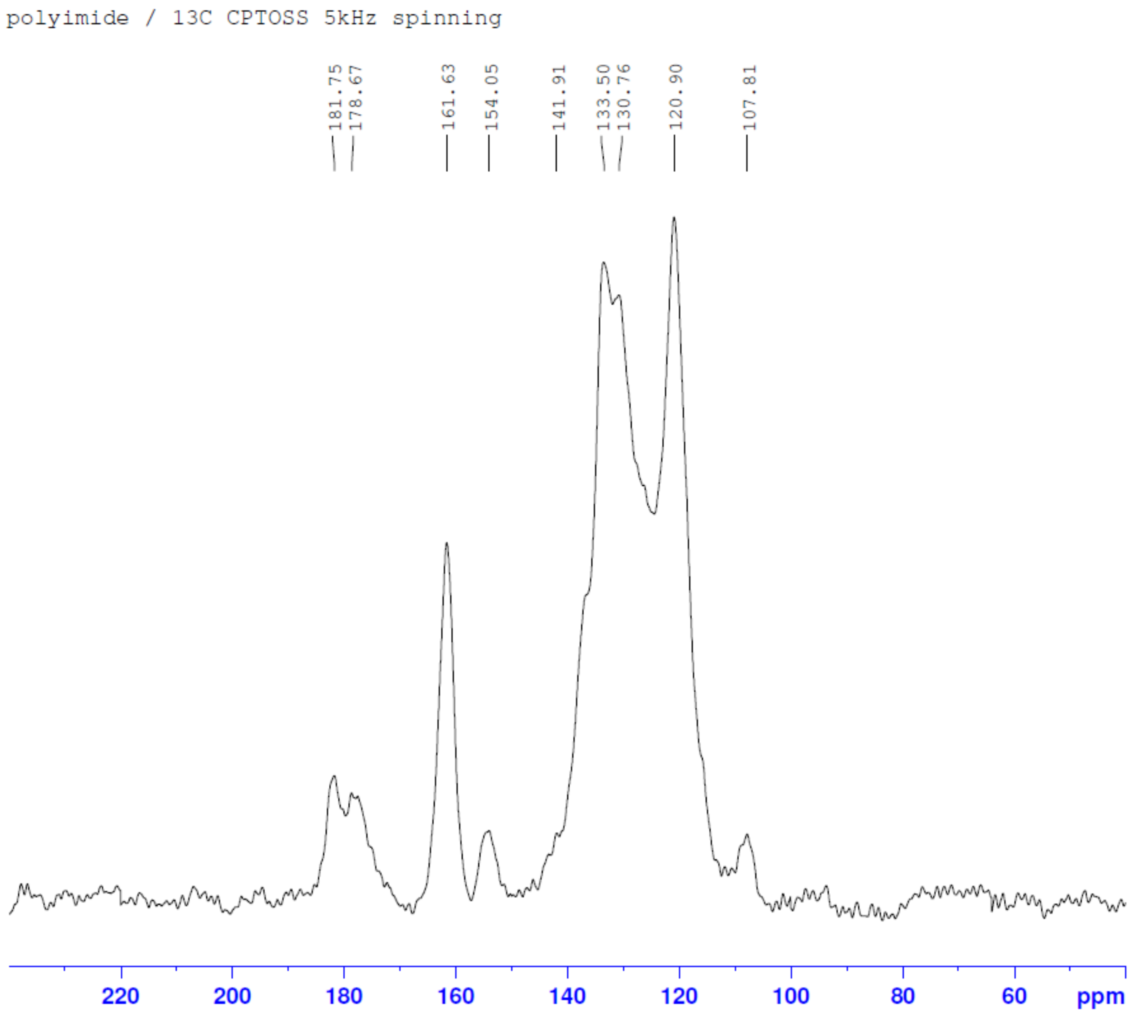

Figure S2. High-resolution regional XPS spectra of (a) C 1 s signals, (b) N 1 s regions, and (c) O 1 s regions of the PI.

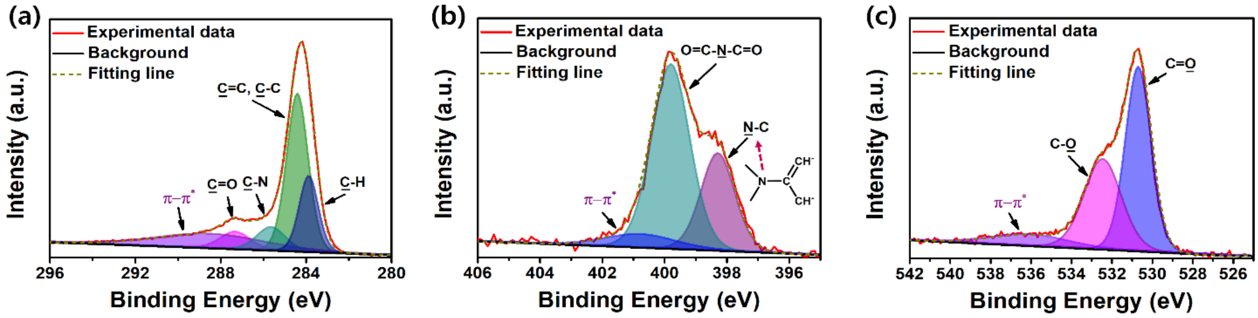

Figure S3. SEM images of the PI powder at the different magnifications (a–c). The FE-SEM images showing the formation of the π-stacked PI aggregated morphology between conjugated perylene cores in the PI.

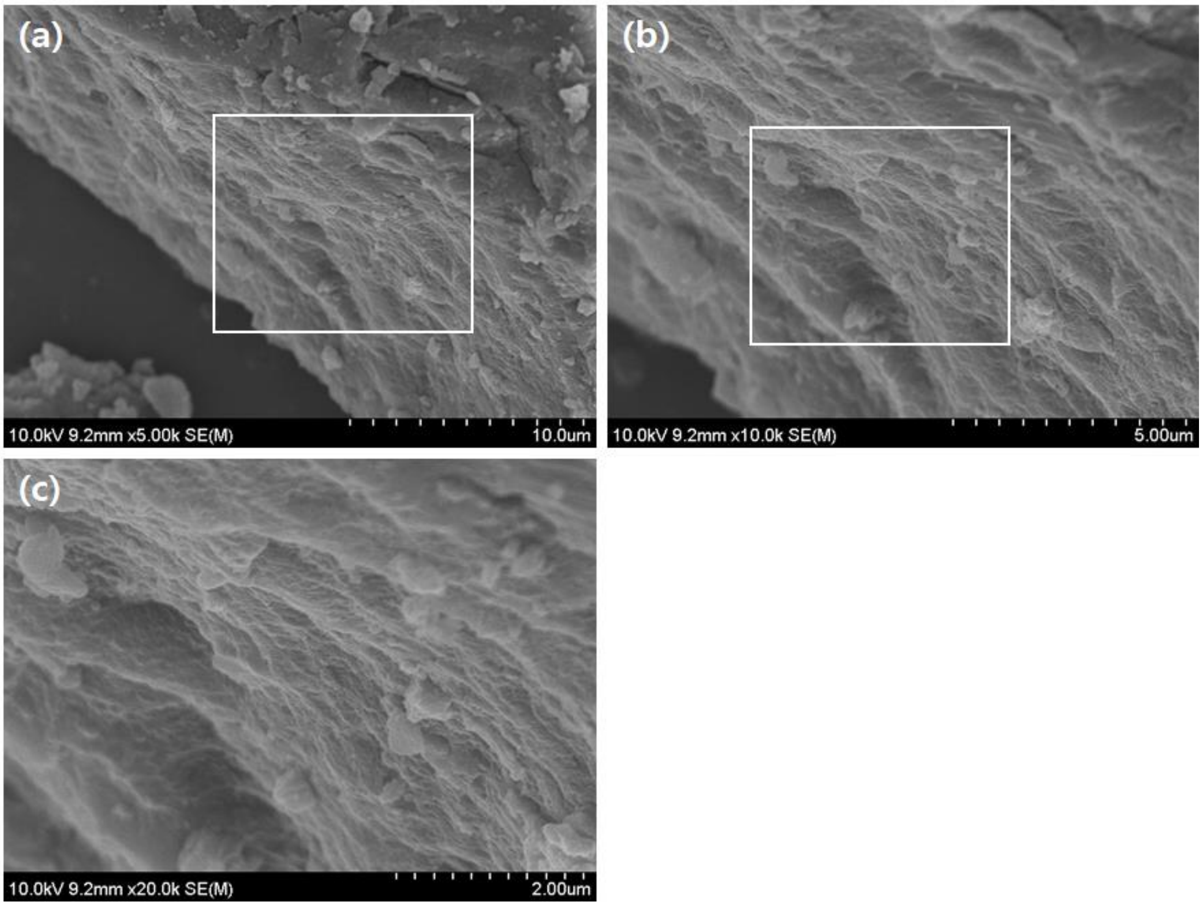

Figure S4. The relationship of square root of scan rate and peak current ($\log i_p$ vs. $\log v$) for (a) PI electrode vs. Li^+/Li at the voltage of 2.0 V; (b) PI electrode vs. Na^+/Na at the voltage of 1.9 V.

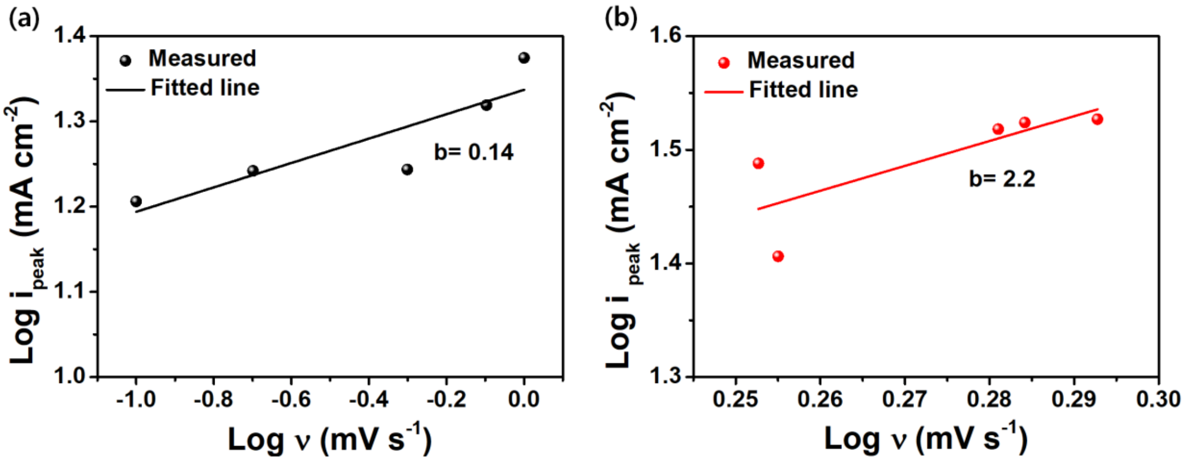

Figure S5. The shadow region shows the CV profile for the charge contribution ratio from the capacitive- and diffusion-controlled charge process of PI (vs. Li^+/Li) at the scanning rate of (a)-(e) 0.1 to 1.0 mV s^{-1}.

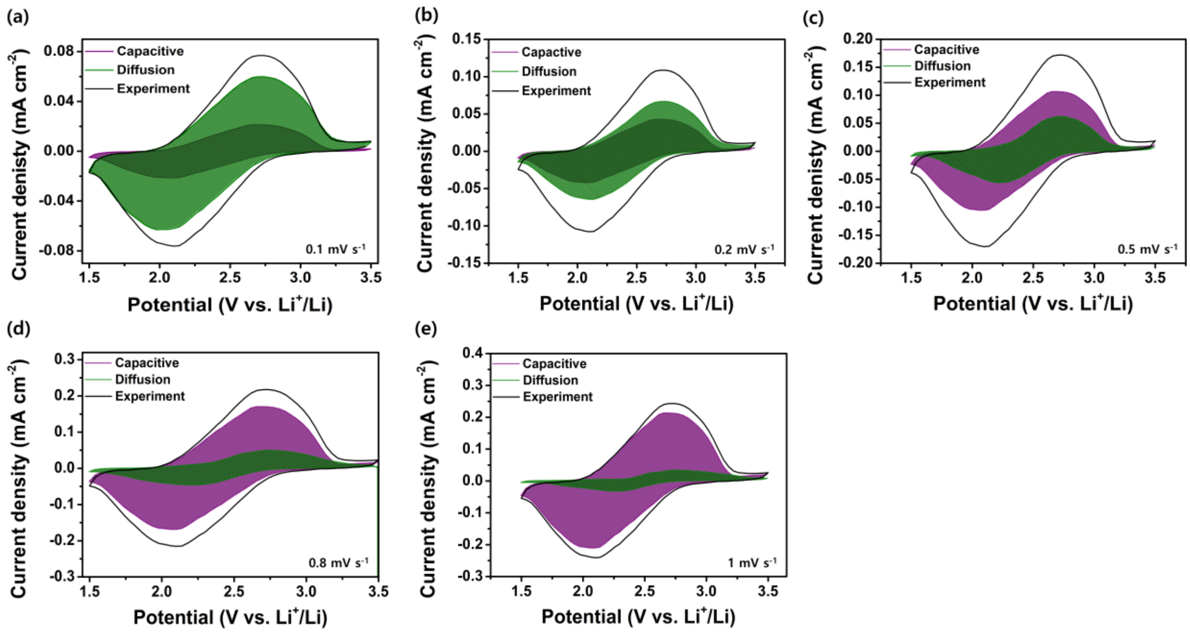

Figure S6. The shadow region shows the CV profile for the charge contribution ratio from the capacitive- and diffusion-controlled charge process of PI (vs. Na^+/Na) at the scanning rate of (a)-(e) 0.1 to 1.0 mV s^{-1}.

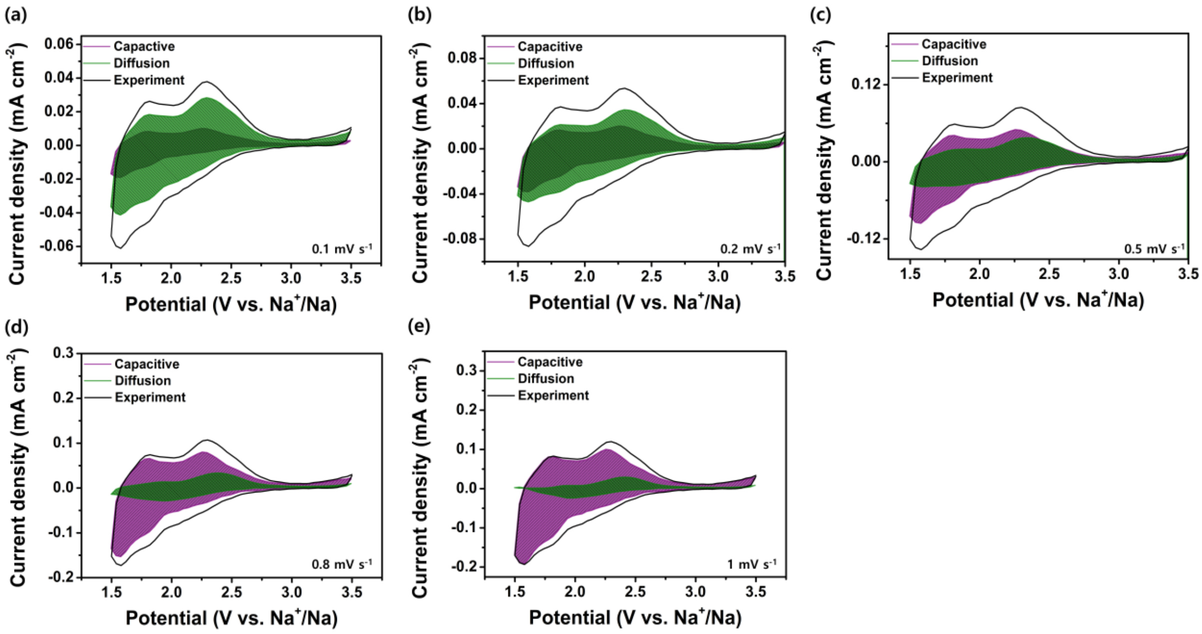

Figure S7. The differential capacity (dQ/dV) vs voltage plots of (a) PI (vs. Li^+/Li), and (b) PI (vs. Na^+/Na) at the current density of 200 mA g^{-1}. Inset shows the extended curves of (b).

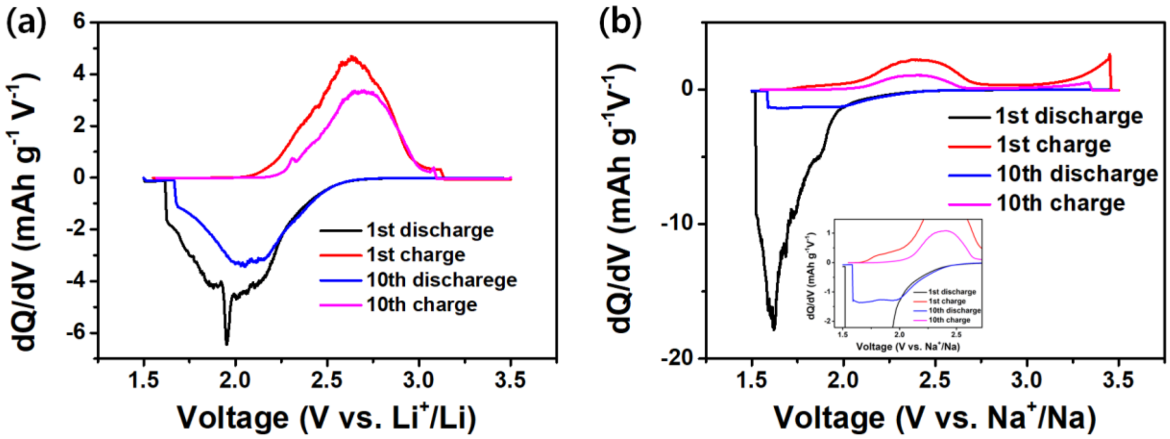

Figure S8. SEM images of (a, b) the pristine PI electrodes; (c, d) cycled PI electrodes for Li^+/Li; and (e, f) cycled PI electrodes for Na^+/Na. Approximately 1000 cycles were conducted at 200 mA g^{-1}.

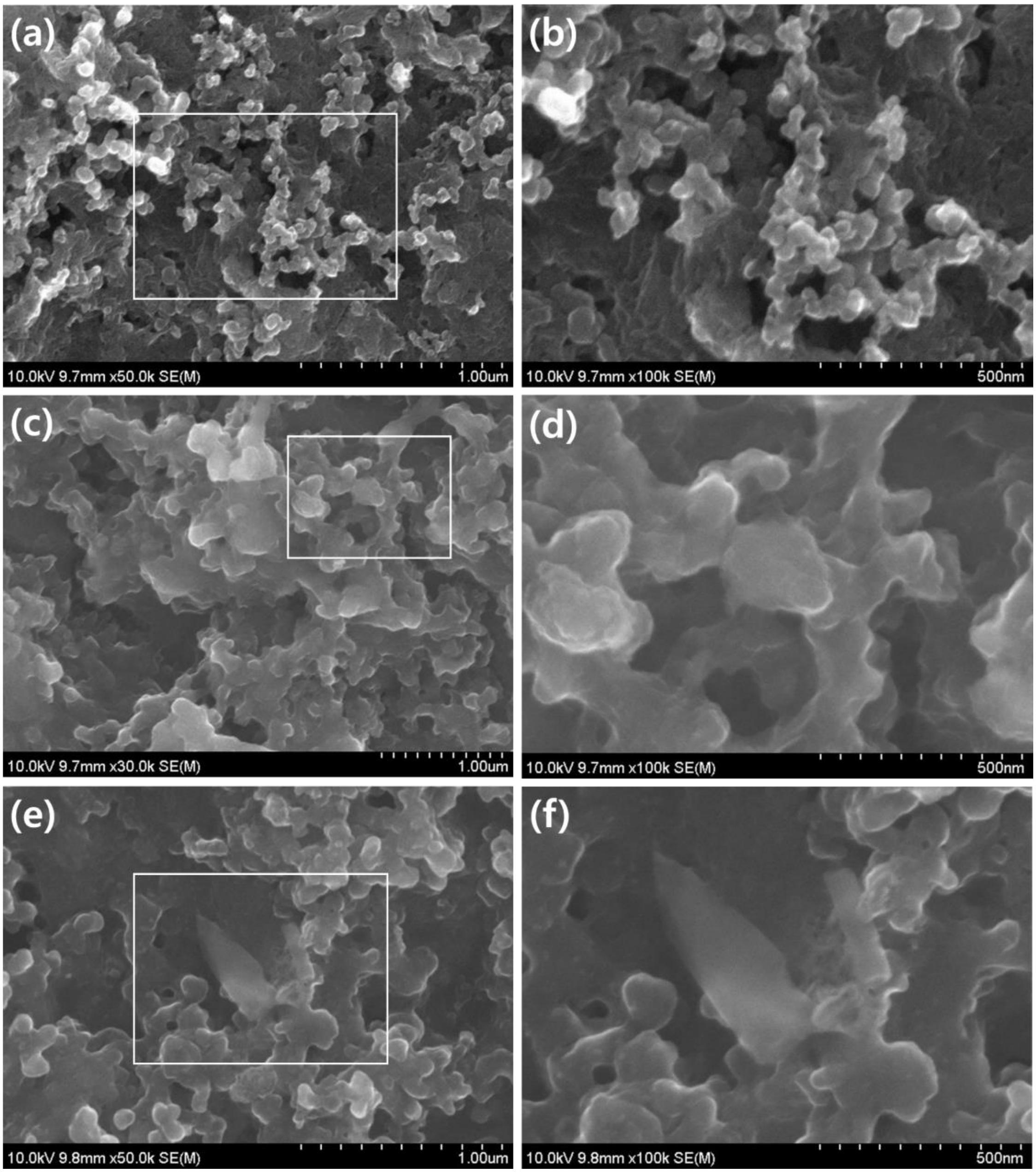

Figure S9. Ex-situ XPS local-scan spectra of N 1s regions for the different states of the PI electrodes (for Li^+/Li and Na^+/Na) after charging to 3.5 V and discharging to 1.5V.

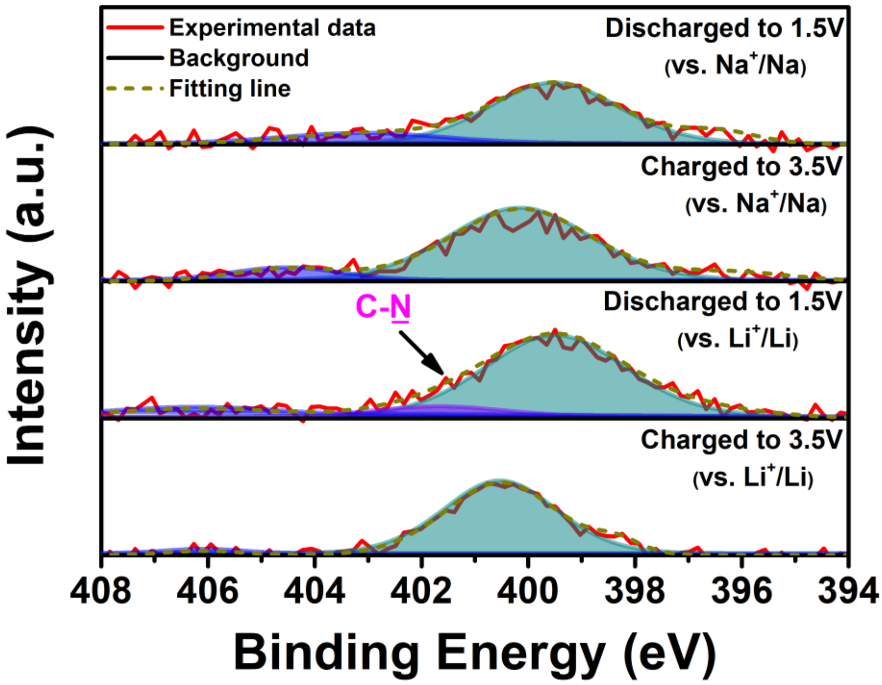

Table S1. Summary of electrolyte resistance (R_e), charge transfer resistance (R_{ct}) for fresh and tested cells at different cycle numbers in both PI-based LIBs and SIBs.

Battery cells	**PI in LIBs**		**PI in SIBs**	
Cycle number	R_e **(Ω)**	R_{ct} **(Ω)**	R_e **(Ω)**	R_{ct} **(Ω)**
0	58.47	392	12.77	272
100 at 200 mA g^{-1}	11.32	337	4.63	243
1000 at 0.5C	61.17	939	49.06	501
1000 at 1C	24.63	573	34.96	390

****